UNIVERSITY OF BIRMINGHAM

University of Birmingham
Research at Birmingham

Processing of glycerol under sub and supercritical water conditions

Tapah, Boris; Santos, Regina; Leeke, Gary

[Link to publication on Research at Birmingham portal](#)

CrossMark

Processing of glycerol under sub and supercritical water conditions☆

B.F. Tapah, R.C.D. Santos, G.A. Leeke*

School of Chemical Engineering, University of Birmingham, Edgbaston, Birmingham B15 2TT, UK

ARTICLE INFO

ABSTRACT

Converting glycerol, a by-product from biodiesel production into useful products and energy could contribute to a positive life cycle for the biodiesel process. One kg of glycerol is produced for every 10 kg of biodiesel and has the potential to be used as a source of H_2, syngas or CH_4 by an appropriate conversion process. Catalytic Supercritical Water Gasification (CSCWG) processing of crude glycerol solutions is one such viable option. Above its critical point [>221 barg, >374 °C], the properties of water, such as the low relative permittivity and high ionic product make it capable of dissolving non-polar organic compounds, allowing for high reactivity, and the ability to act as an acid/base catalyst. In this work, the degradation of glycerol by CSCWG at temperatures [400–550 °C] and pressures [170–270 barg] was investigated using a packed bed reactor (PBR) containing a $Fe_2O_3 + Cr_2O_3$ catalyst. Glycerol feed concentrations were between 2 and 30 wt% at flow rates from [10–65 ml/min], which gave weight hourly space velocities (WHSV) of [38–125 h^{-1}]. The results indicated that high temperature and low feed concentration tended to increase the gas yield and selectivity toward H_2 production with some char (<2.7 wt%). Syngas of up to 64 mole% was obtained with minimum 4:1 mole ratio of H_2:CO. High yields of volatile hydrocarbons were also obtained: 14 and 69 mole % for methane and ethylene, respectively, which could be used for energy generation in SOFCs or turbines, reformed to syngas or converted to chemicals by an appropriate route. Pressure had little effect on the gas yields in the subcritical water region, but had a positive effect on H_2 and CO_2 in the supercritical region where char formation also was increased resulting in loss of catalyst activity. Complete conversion of glycerol was achieved at high temperature (550 °C). A maximum of 11 wt% liquid products were obtained at 400 °C (mainly allyl alcohol, methanol and formaldehyde). Catalyst stability was also evaluated, which was found to reach relative stability in the supercritical water environment for up to 9 h of operation.

1. Introduction

The world continues to explore alternative source of energy and chemicals in order to reduce dependency on fossils fuels and to ensure the security of energy supply. Biodiesel production could play a significant role in this process. Large amounts of glycerol are obtained as waste products from biodiesel production, with about 1 kg of glycerol produced for every 10 kg of biodiesel. In 2009, the biodiesel product from the European Union and United States reached a massive share of 9 and 2.7 million tons respectively, from a total of 16 million tons worldwide. 1.6 million tons of glycerol was

therefore, produced as an obligatory by-product [1]. Glycerol can be used as an ingredient in various fields, for example, in the food industry as humectants, solvents and sweeteners, and also in the medical, pharmaceutical and cosmetic industries, but the demand for glycerol in these processes is limited. Raw glycerol obtained from biodiesel manufacture contains impurities, and its purification process will, therefore be costly due to the requirement of separation units, which require energy input. However, crude glycerol is widely available and cheap and offers new opportunities for chemistry and energy use [2,3].

Catalytic supercritical water gasification (CSCWG) is a promising route in which organic material can be efficiently decomposed to produce a mixture of gases and value-added liquid products depending on the process conditions [4]. The gas mixture can contain hydrogen, carbon monoxide, carbon dioxide, methane, ethylene, and the liquid fraction, can contain value added products (e.g. acetaldehyde, acetic acid, acetone, methanol and ethanol); char can also be obtained [5,6]. Water, above its critical point [≥221 barg, ≥374 °C], has low relative permittivity (6 compared to
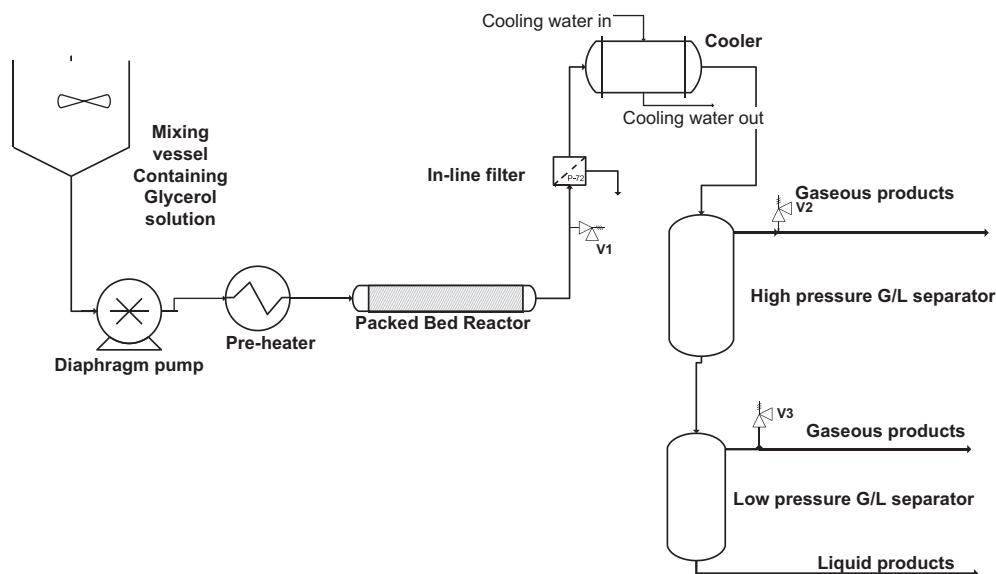
Fig. 1. Simplified Process Flow Diagram of CSCWG Equipment.

80 at ambient), high ionic product (10^{-11} as compared to 10^{-14} for subcritical) [7], which can be manipulated by changing pressure and temperature. These properties offer a number of advantages for organic material decomposition, such as enhanced capability to dissolve non-polar compounds, high reactivity and the ability to act as an acid/base catalyst.

The production of hydrogen and/or syngas by supercritical water processing of crude glycerol solutions has been reported in the literature [8–14,35]. The selectivity of the process toward either H_2 or syngas ($H_2 + CO$), or CH_4 can to some extent be steered by tuning the process conditions and by catalyst selection [15,16]. Several heterogeneous catalysts have been studied to promote hydrogen yield and to reduce the formation of tars and char during CSCWG reaction, such as Ru and Rh [17,18]. However, the aim of this work is to combine the utilisation of an effective and low cost catalyst (iron oxide based) at temperatures up to 550 °C, to attain conversion of glycerol to gaseous products, which has not been reported in the literature to date. Under less severe conditions, conversion of glycerol to value added liquid products is also expected. The effects of temperature, pressure, feed concentration, WHSV and time online on the product gas yields are reported.

2. Materials and methods

2.1. Materials

Glycerol (99% purity) was purchased from Sigma Aldrich, UK and was used without further purification. Deionised water was used to prepare a range of glycerol concentrations [2, 5, 10, 15, 20, 30 wt% glycerol]. The catalyst (Catal CT 54) was supplied by Catal International Ltd and was a mix of unsupported iron oxide: chromium oxide (91:9 wt% respectively) with spherical particles of 4 mm diameter and Brunauer-Emmett-Teller (BET) surface area of 58 m^2/g, as measured. Chromium was blended with the iron to stabilise the oxide element on its surface by promoting oxidation resistance. This catalyst is reported to be capable of withstanding extended steaming without loss of its mechanical strength, and it is suitable for high temperature (HT)-WGS reactions for the conversion of CO in reformate streams.

Gas standards for gas chromatography (GC) analysis were obtained from Scientific and Technical Gases Ltd, UK and were composed of a mixture of hydrogen, carbon dioxide, carbon monoxide, methane, ethane and ethylene with nitrogen balance gas. Liquids standards for GC analysis (methanol, ethanol, ally alcohol, formaldehyde, acetaldehyde, valeraldehyde, acrolein), were purchased from Sigma Aldrich, UK.

2.2. CSCWG reactor set-up and methods

The CSCWG experiments were carried out in a Hastelloy C276 tubular reactor with the following dimensions: OD Tube = 25.2 mm with a wall thickness of 3.2 mm, length of 11 cm, empty volumetric capacity 30.5 cm^3. The working conditions for the reactor system were 600 °C at 300 barg. The reactor was packed in-house with 32.1 g of catalyst to fully fill the reactor bed. The integrity of the packing was validated using a HPLC spike method which resulted in a chromatogram with a Gaussian response. This indicated that the packing was uniform. The experimental rig was first flushed with water, and the system pressure was increased to the desired condition. The reactor temperature was set and controlled by a Parr controller (Model 4843). The temperature of the system was measured (± 0.1 K) with four Type K thermocouples with one of the thermocouples directly measuring the reactor temperature. Water was passed through the reactor and ancillaries for 40 min in order to equilibrate the system before the glycerol solution was introduced at the desired flow rate by a high pressure diaphragm pump (Lewa LCD1, GmBh). The product stream leaving the reactor was cooled to approximately 30 °C using a shell and tube heat exchanger. A pressure regulator was used to maintained the desired upstream reactor pressure and the pressure in the downstream high pressure gas–liquid separator, where gas was separated from the condensed liquid. A second downstream low pressure separator (at approximately 20 barg) was used to maximise the gas–liquid separation. Gas and liquid products samples were collected after the first 5 min and thereafter every 15 min. A simplified schematic of the process is shown in Fig. 1.

2.3. Analytical methods for the gaseous products

Analysis of the gaseous products was undertaken by gas chromatography using Agilent 6890N GC equipped with thermal conductivity detector (TCD) and a micro-packed column [Restek Shincarbon 100/120 ST column (length 2 m, ID = 1 mm)]. Helium was used as carrier gas at a flow rate of 11.3 ml/min. The oven
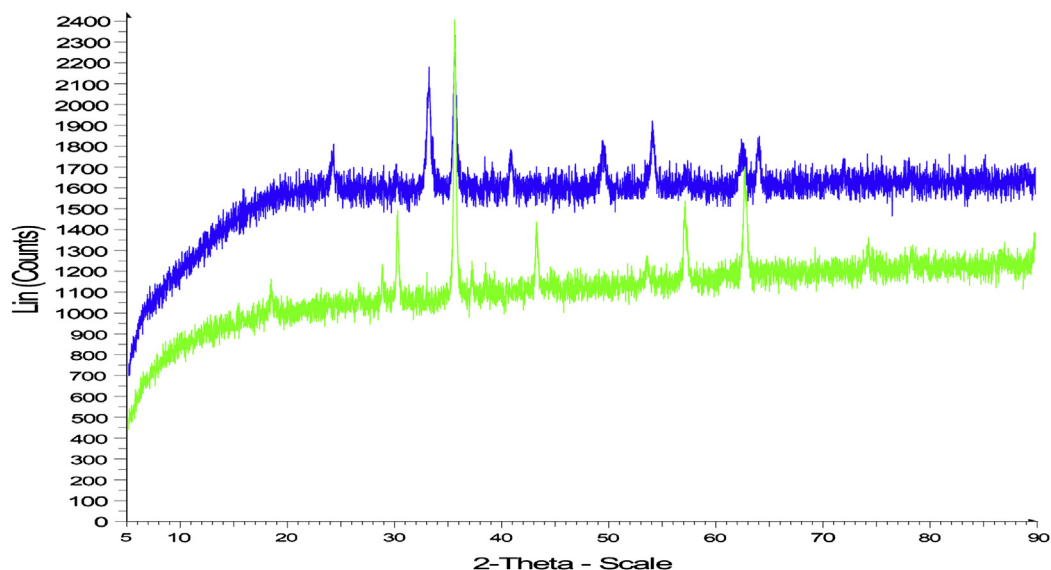
Fig. 2. XRD patterns of fresh (a) and used (b) samples of non-supported Fe_2O_3 + Cr_2O_3 catalysts. ■ (a) Fresh, ■ (b) Used. *Fresh Catalyst 2 theta values: 32 Cr, 35 Fe, 39 Cu, 50 Al, 54 Si, and 63 Ca. Used Catalyst 2 theta values: 30 Cr, 35 Fe, 42 Cu, 54 Al, 57 Si, and 63 Ca.* The Fe_2O_3 Powder Diffraction Data were analysed by comparing data to the indexed diffraction pattern for $CrFe_2O_3$ found in the JCPDS database [38], Miller indices (h k l; indicating the set of lattice planes responsible for that diffraction peak) were assigned to each peak in the diffraction pattern as shown below.

2θ	32.8	35.4	39.9	50.4	54.3	57.7	63.8
h k l	1 0 0	1 1 0	1 1 1	2 0 0	2 1 0	2 1 1	2 2 0

temperature was initially held for 8 min at 40 °C, and then the temperature was increased at 50 °C/min up to 250 °C. The detector temperature was 250 °C. A gas syringe of 2.5 ml capacity was used to introduce the gas sample into the GC system through a packed inlet and 6-port pneumatic sampling valve, equipped with 2 ml loop. The chromatogram peaks of the gas products were identified by comparing the retention time of the sample peaks with the gas external standard. The concentrations of each of the gas components in the sample ($C_{g, i}$) were determined from equation (1) (nomenclature is given in after 'Conclusions'):

$$C_{g, i} = \frac{Ag, i}{As} * C_s \qquad (1)$$

2.4. Characterisation of the Fe_2O_3–Cr_2O_3 catalyst

A Micromeretics instrument (Model ASAP2010) was used for BET surface area and porosity measurements of the fresh and used samples of the catalyst. Nitrogen adsorption/desorption at 77 K was used and the micropore diameter was estimated using the Barrett–Joyner–Halenda method applied to the desorption side of each isotherm. An emission scanning electron microscope (ESEM), model XL30 (FEI company) was operated with back scatter electron (BSE) detector and associated energy-dispersive spectrometer (EDS) equipped with X-ray detector, and was used to perform visual and chemical characterisation of the catalyst samples. X-ray diffraction was performed to determine the physical profile of the sample (using a Siemens model D5005) with 2.2 kW sealed Cu Source operated at 20 kV, 30 mA and equipped with a scintillation counter detector. These analyses were recorded over the 2θ ranging from 5 to 89° at a scan rate of 0.015°/min.

3. Results and discussion

Catalytic supercritical water gasification (CSCWG) of glycerol was undertaken to study the effects of process parameters on the composition and yields of gas products; process parameters included temperature, pressure, glycerol feed concentration, WHSV and time online. The investigations were undertaken between 400 and 550 °C and 170 to 250 barg with glycerol feed concentrations at 2, 5, 10, 15, 20, 30 wt%. The main products of CSCWG of glycerol in the presence of the mixed iron oxide: chromium oxide catalyst was identified as a mixture of gaseous products (hydrogen, carbon monoxide, carbon dioxide, methane, ethylene) and liquid products that contained alcohols (methanol, ethanol and allyl alcohols), aldehydes (formaldehyde, acetaldehyde, propionaldehyde, allyl aldehyde, valeraldehyde). The distribution of products in this work is similar to those reported by other researchers [4,5,17,18] using Rh, Ni, Ru/ZrO_2 and Ru/Al_2O_3 catalysts with the exception of hydroxyacetone and acrylic acid.

3.1. Catalyst characterisation

The fresh and used catalysts (after 172 h on-stream) were analysed using powder XRD, and the results are shown in Fig. 2 with the assignations of the main 2 theta values. The patterns of the fresh and used samples of Fe_2O_3 + Cr_2O_3 were significantly different as seen by the change in peak location, height and intensity of the patterns (note that the same mass of 0.51 g was used for both samples). The patterns reveal a relatively poor crystalline structure. Energy Dispersive Spectroscopy (EDS) was undertaken to determine the chemical composition of the catalyst surface. ESEM images of the fresh (a) used (b) samples of the catalysts are shown in Fig. 3a and b, respectively. The surfaces of both catalysts exhibit some porosity as also confirmed by the range of pore sizes detailed in Table 1. The presence of score marks can be seen on both images (a and b) and may have occurred during catalyst preparation, where pellets were crushed to pass through a 200 micron sieve, before mixing with of 1% graphite, in order to obtain a final pellet. It can be seen in image (b) that the structure fragmented into smaller particles. This could be due to sintering of the catalyst under supercritical water (SCW) conditions [19]. This thermal degradation of the catalyst may have contributed to a progressive loss of activity (refer to Section 3.3.3).

Surface area, pore volume and pore size of the catalyst samples was determined from BET measurements, and the results are
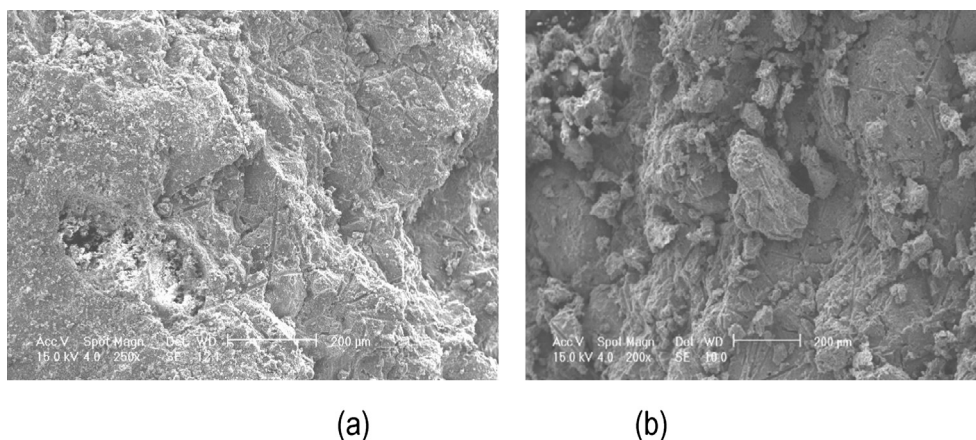
Fig. 3. ESEM images of the fresh (a) and used samples (b) of Fe_2O_3 + Cr_2O_3 catalyst. Images are at the same scale of 200 μm.

shown in Table 1. The BET surface area of the catalyst was initially 58.1 m^2/g and was reduced to 25.8 m^2/g in the used sample. This significant decrease may have resulted from sintering of the catalyst and erosion under SCW conditions as evidenced in Fig. 3b. A significant increase in the micropore area from 0.03 to 2.06 m^2/g may have resulted from the formation of new micropores within the catalyst. It is expected that SCW will act as strong oxidant, which could promote the reactivity and diffusion rate of the gases on the catalyst, resulting to the formation of pores. On the other hand, the presence of impurities and char on the surface of the catalyst would concomitantly reduce the micropore area. The slight increase in the total nanopore volume of the fresh and used samples (0.21 and 0.23 cm^3/g respectively) and the minor change to the micropore volume (0.0006 and 0.0007 cm^3/g, respectively) suggest that pore blockage and filling from coke deposition was negligible. ESEM-EDS was used to quantify coke deposition and the results are discussed in Section 3.3.3.

3.2. Effect of temperature on the non-catalytic gasification of pure glycerol

A series of gasification experiments without catalyst were conducted for 15 wt% glycerol, at different temperatures to assess the influence of gasification temperature on product gas composition and yield as shown on Figs. 4 and 5.

Temperature has a significant influence on the product gas yield and composition, as expected. The overall gas product increased with temperature from 67 to 76 wt% for 400–550 °C, respectively (Fig. 4). This is attributed to thermal cracking of glycerol into gaseous products. The formation of a mixture of gases containing: H_2, CO, CO_2, CH_4 and C_2H_4 (Fig. 5) resulted from the variety of reactions that occur in this process, e.g. hydrocarbon cracking, water gas shift (WGS) and methanation. It can be seen that when the temperature increased from 400 to 550 °C, H_2 and CO_2 yield increased from 13 to 28 mole % and 4–14 mole % respectively. The CO yield increased from 6 to 18 mole% over the same temperature range.

CH_4 yield is 19 mole % at 400 °C, but declines to 10 mole% at 550 °C. This indicated that CH_4 formation was favoured at lower temperature while high temperature can promote methane reforming to the benefit of H_2 production in SCW conditions. Similarly, ethylene yield declines from 58 to 30 mole %, which would have resulted from cracking under increasing temperature. The catalytic effect of the hastelloy reactor should, however, not be disregarded [20].

3.3. Effect of process conditions on the catalytic gasification of pure glycerol

High temperature favours gas production, however, a viable and economical process will need a suitable catalyst in order to achieve higher gasification yields at lower temperatures and optimal WHSV. In this section, a series of experiments were carried out at various conditions (WHSV, pressure, temperature, feed concentration and time on-line) in the presence of Fe_2O_3 + Cr_2O_3 catalyst to study their effect on gas yields.

3.3.1. Effect of WHSV

Gas product analysis at the reported conditions shows that the main products were H_2, CO, CO_2, CH_4, and C_2H_4. The effect of WHSV appears to increase the selectivity toward H_2 and CO yields as shown on Fig. 6. Note Fig. 6 has a log *y*-axis for clarity.

It is evident that H_2 yield increases sharply from 17 to 34 mole % when WHSV increases from 19 to 125 h^{-1}. Similarly CO increases from 3.1 to 7.8 mole % for the same range of WHSV. This may be due to reactions such as $C(s) + CO_2 \rightarrow 2CO$ (Boudouard, $\Delta H_R = +172.4$ kJ mol^{-1} and/or $CH_4 \leftrightarrow C_{(S)} + 2H_2$, ($\Delta H_R = +74.8$ kJ mol^{-1}). CO_2 increases from 4.8 to 5.5 mole % when WHSV increases from 19 to 73 h^{-1}, and remains fairly constant from 73 to 125 h^{-1}.

Ethylene yield was 69 mole % at WHSV of 19 h^{-1}, but decreased steadily to 45 mole % at a WHSV of 125 h^{-1}. At the same time,

Table 1
Catalyst surface area, pore volume and pore size.

| Properties		Fresh sample	Used sample after 172 h on-stream
Area			
BET surface area:	m^2/g	58.1	25.8
Langmuir surface area:	m^2/g	80.4	35.8
Micropore area:	m^2/g	0.03	2.1
External surface area:	m^2/g	58.1	23.8
Volume			
Single point adsorption total pore volume of pores less than 1084.5096 Å diameter at P/Po 0.98197675:	cm^3/g	0.21	0.23
Micropore volume	cm^3/g	0.00063	0.00073
Pore size			
Adsorption average pore diameter (4V/Å° by BET):		151.3 Å°	364.4 Å°
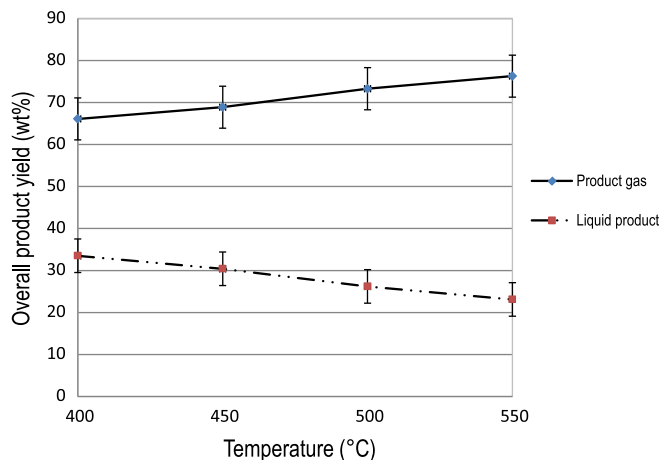
Fig. 4. Gas and liquid product yields for non-catalytic SCWG of 15 wt% glycerol. $P = 250$ barg at $F = 65$ ml/min, $\tau = 28$ s.

Fig. 6. Effect of WHSV on CSCWG of 20 wt% glycerol. $T = 500$ °C and $P = 250$ barg.

methane yield also decreases from 9.4 to 8.7 mole % and is attributed to improved contact (due to higher turbulence) of the reacting medium over the catalyst active sites, which seem to favour catalytic cracking of hydrocarbons at shorter residence times. The high yield of ethylene at lower WHSV (19–73 h^{-1}), could be due to poorer mixing, and demonstrated that iron based catalysts could be commercially utilised for the production of hydrocarbons [21,22] at lower WHSV. The overall gas yield is moderately high at 76 wt% when WHSV is 125 h^{-1} (refer to Fig. 11), which resulted from uniform reactant distribution throughout the reactor bed, whereas when WHSV is 73 h^{-1} with similar conditions, the overall gas yield is reduced to 65 wt% (Figure not shown). Thus, the product distribution (gas and liquids) is therefore dependent on the flow rate and catalyst weight.

3.3.2. Effect of pressure

The effect of pressure was studied between 170 and 270 barg (below and above the critical pressure of water) and was found to have a small effect on the gas composition (H$_2$, CO, CO$_2$, CH$_4$, C$_2$H$_4$) and yield below the subcritical region (<221 barg), except for H$_2$ and C$_2$H$_4$, as shown on Fig. 7. A positive pressure effect was noticeable in the supercritical region, which resulted in the increasing yields of H$_2$, CO and CO$_2$ coupled with a slight decrease in the hydrocarbons.

At subcritical conditions, H$_2$ yield increases with pressure from 37 to 52 mole %, while CO yield remains relatively constant at 2 mole %. The increases in H$_2$ and CO$_2$ yields with increasing pressure are attributed to the promotion of the WGS reaction. However, unidentified side reactions could occur also, as evidenced by the small increase in CO yield in the supercritical region, which became noticeable under the influence of high pressure. The ionic product of water increases with increasing pressure, therefore, the hydrolysis reaction that plays a significant role in CSCWG also increases. CO$_2$ yield increases from 4 to 7 mole % when the pressure crossed the supercritical water region, which further indicates that the WGS reaction is favoured, an observation similar to other research findings [23]. The process can be operated at an optimal pressure to enhance the gas selectivity in order to either maximise H$_2$, CH$_4$ or syngas yields.

Methane yield was relatively low (∼ 6 mole %) in subcritical conditions, but it increased to 11 mole % in the critical regions, whereas ethylene yield was 51 mole % at low pressure (170 barg) and decreases sharply to 28 mole % at high pressure (270 barg), which may indicate its reformation under supercritical water conditions. It has been reported that using a suitable metal based catalyst and moderate temperature (<500 °C) and pressure (>71 barg), ethylene can be reformed into ethanol [24,25] as shown by equation (2). Evidence of increasing ethanol yield in the in liquid
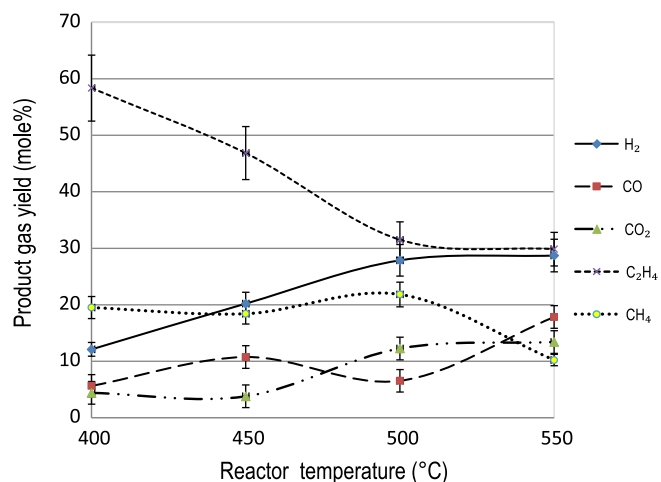

Fig. 5. Gaseous products identified from the non-catalytic SCWG of 15 wt% glycerol. $P = 250$ barg at $F = 65$ ml/min, $\tau = 28$ s, LHSV = 128 h^{-1}.
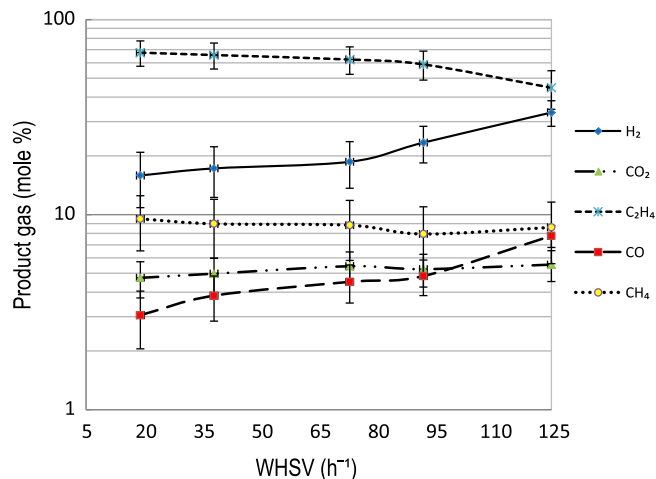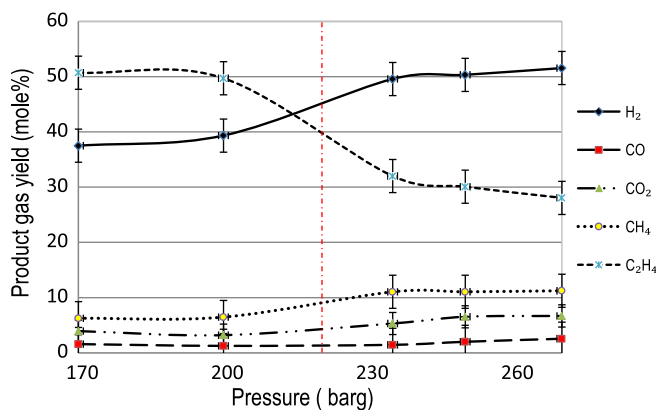

Fig. 7. Effect of pressure on gas product yield for 10 wt% glycerol. $T = 500$ °C, WHSV = 125 h^{-1}. Vertical dotted red line indicates supercritical conditions at 221 barg. (For interpretation of the references to colour in this figure legend, the reader is referred to the web version of this article.)
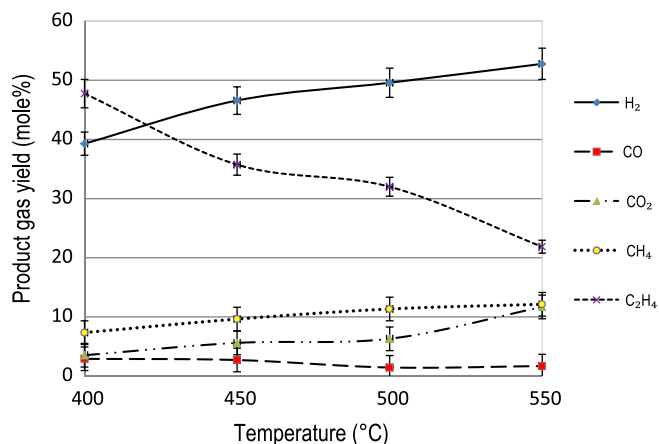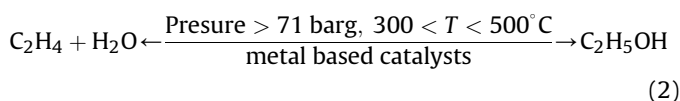
Fig. 8. Effect of temperature on gas products yield for 10 wt% glycerol. $P = 235$ barg, WHSV $= 125$ h^{-1}.

Fig. 10. Effect of glycerol feed concentration on gaseous products. $T = 500\,°C$, $P = 235$ barg and WHSV $= 125$ h^{-1}.

samples was observed (results are presented in a separate paper, but are introduced in Section 3.4).

$$C_2H_4 + H_2O \xleftarrow{\text{Presure} > 71 \text{ barg}, \ 300 < T < 500°C}_{\text{metal based catalysts}} \rightarrow C_2H_5OH \tag{2}$$

3.3.3. Effect of temperature

The influence of reactor temperature between 400 and 550 °C was studied to evaluate gas yields, and to maximise the overall gaseous product. The results are shown on Figs. 8 and 9.

It can be seen in Fig. 8 that H_2 yield increases at a low rate from 39 to 53 mole %, while CO_2 yield is initially low (4 mole %) at 400 °C, but increases to 12 mole % at 550 °C, which may be attributed to the activity of the WGS reaction. Ethylene decreases from 48 to 22 mole % when temperature increases 400–550 °C respectively, and can be attributed to thermal cracking at higher temperature (also seen in Section 3.2). On the other hand, methane yield is low (8 mole %) at 400 °C, but increases slightly to 12 mole % at 550 °C. This could be due to the effects of side reactions, such as methanation and cracking of C_2H_4. Loss of catalyst activity would also favour side reactions, such as methanation ($3H_2 + CO \rightarrow CH_4 + H_2O$) and polymerisation of ethylene to form coke. After 172 h on-stream a dark/black colour material deposited on the inside of the reactor wall was identified as coke by ESEM-EDS analysis; the fresh and
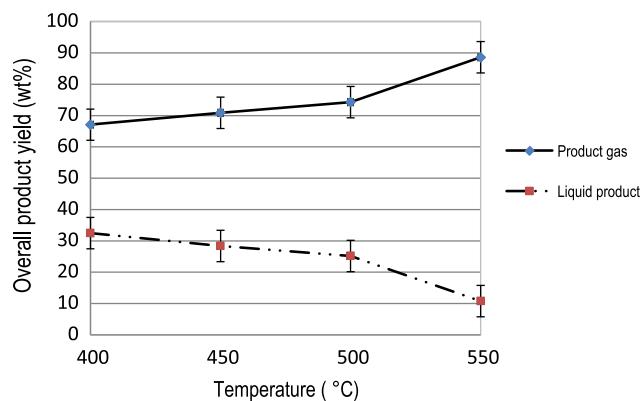
used samples, gave carbon dry catalyst weights of 4.5 and 7.2 wt%, respectively; representing 2.7 wt% carbon (refer to Table 2). The accumulation of carbon on the catalyst surface could contribute to the consumption of hydrogen through gas–solid reactions i.e. $C + 2H_2 \rightarrow CH_4$ ($\Delta H_R = -74.8$ kJ mol^{-1}). This reaction is exothermic and consequently, temperature has a negligible effect on its formation. Some researchers have reported that methane selectivity could be 40–60 mole % for supported Fe [26], and as high as 95 mole % when the temperature is between 350 and 550 °C [26,27]. Other studies using Ni and Ru catalysts have revealed that low temperature and high pressure favour the formation of CH_4, but reduce the decomposition reaction rate of glycerol [6]. In contrast, high temperature (associated with a low pressure regime) favoured the formation of H_2 and CO. In light of this, and the results shown in Figs. 5 and 8, the hydrocarbon yield can be attributed to the catalyst choice, catalyst activity and reaction conditions (particularly temperature) in CSCWG.

At 400 °C, syngas (H_2:CO) yield was ~42 mole % and increased to 55 mole % at 550 °C. Syngas yield was high because of improved H_2 yield and as a result, H_2:CO ratio increased from 13:1 at 400 °C to 26:1 at 550 °C. Water in the CSCWG process would have promoted the WGS reaction ($\Delta H_R = +41.0$ kJ mol^{-1}) and decreased CO concentration. The reverse-WGS ($CO_2 + H_2 \rightarrow CO + H_2O$; though this is less thermodynamically favoured at higher temperature $\Delta H_R = -41.0$ kJ mol^{-1}) and/or $C(s) + CO_2 \rightarrow 2CO$ may have contributed in CO formation as suggested in other findings [29–31],

Fig. 9. Effect of temperature on gas–liquid product yields for 10 wt% glycerol. $P = 235$ barg, WHSV $= 125$ h^{-1}. Note gas and liquid yields do not equal 100% as char formed part of the overall product.
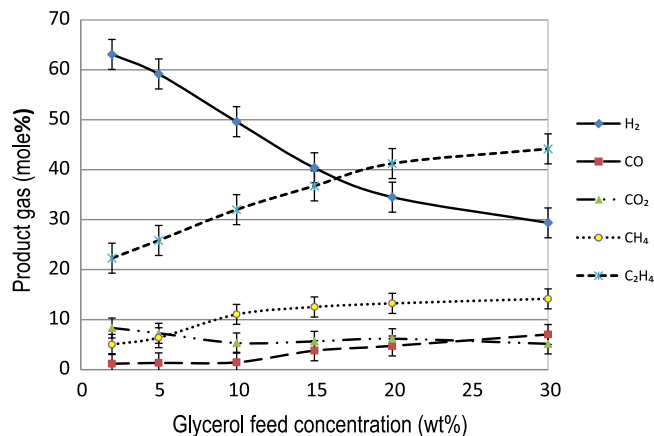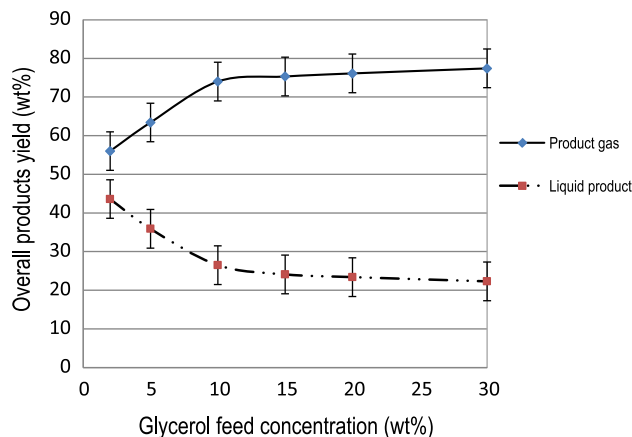

Fig. 11. Effect of glycerol concentration on gas–liquid product yields. $T = 500\,°C$, 235 barg and WHSV $= 125$ h^{-1}.

Table 2
EDS data of the fresh (a) and used samples (b) of Fe_2O_3 + Cr_2O_3 catalyst.

Element	Weight %	Atomic %
(a) Fresh Fe_2O_3 + Cr_2O_3		
C K	4.6	14.8
O K	10.5	25.6
Al K	0.3	0.5
Si K	0.4	0.5
Ca K	0.3	0.3
Cr K	5.9	4.4
Fe K	75.6	52.5
Cu K	2.4	1.4
Totals	100.00	
(b) Used Fe_2O_3 + Cr_2O_3 (after 172 h)		
C K	7.2	20.9
O K	12.5	27.3
Al K	0.7	0.9
Si K	1.3	1.6
Ca K	1.1	0.9
Cr K	6.8	4.6
Fe K	67.7	42.3
Cu K	2.7	1.5
Totals	100.00	

where Fe/Cu and Ru/Ni catalysts were used. These types of side reactions are known to occur if the catalyst losses its activity. Fig. 9 shows that the overall gas yield increases from 67 wt% at 400 °C to 89 wt% at 550 °C; meanwhile the liquid product decreased from 35 wt% to 10 wt%, respectively. It is worth noting that gas yields are higher than those obtained without Fe_2O_3 + Cr_2O_3 catalyst (refer to Fig. 4). The increase of gas yield is due to catalytic cracking and thermal cracking of glycerol (and liquid products) as the temperature increased. At 550 °C, complete conversion of glycerol was achieved as evident by the absence of glycerol in the analysed liquid sample, whereas 49 wt% of unconverted glycerol was present in the sample at 400 °C. It should be noted that continued operation at ≤400 °C for feed concentrations greater than 50 wt% glycerol, resulted in plugging of the reactor as a result of coke formation. This problem, however, could be alleviated by raising the temperature above 500 °C. It has been suggested that at lower temperatures the reaction rates for coke formation are higher than the rates of reforming and carbon gasification [32,33]. At temperatures, <450 °C lower gas yields were obtained due to poor conversion of reactants and the reduced role of the WGS reaction. Other works have revealed that low temperature could also result in a less clean product gas, which is likely to contain various amounts of light hydrocarbons, such as C_2H_2 and C_2H_4, as well as up to 10 wt% heavy hydrocarbons, the latter condense to form tar [28,34]. This is also true in this work with the exception of C_2H_2, which was not observed. Tar is obviously an undesirable by-product of CSCWG as it can block valves, in-line filters and interfere with conversion processes.

3.3.4. Effect of glycerol concentration

Feed concentration is a key parameter for the economical evaluation of the gasification process. It is essential to use only the necessary amount of feed in order to achieve optimum yields. The effect of glycerol feed concentration was studied from 2 to 30 wt% at WHSV = 125 h^{-1}, P = 235 barg and T = 500 °C, and the results are shown in Figs. 10 and 11.

It can be seen in Fig. 10 that increasing feed concentration from 2 to 30 wt%, results in decreasing H_2 yield from 62 to 29 mole%. CO_2 also decreases from 9 to 6 mole % while CO yield increases from 2 to 7 mole % with the same range of feed concentration, which may point to the reduced role of the WGS due to high carbon to water feed concentration. This would give less water to promote H_2 formation and also char reforming is likely to increase

$(C_{(s)} + CO_2 \rightarrow 2CO$ [35,36]). Syngas decreased from 64 to 36 mole % with increased glycerol feedstock concentration. This is largely due to decreasing H_2 yield, which affected H_2:CO ratios. As a result, the ratio decreased significantly with increased glycerol concentration from 31:1 to 7:1 to 4:1 for 2, 15 and 30 wt% respectively. Lowering the feed wt% enhances the gasification process by efficient heat transfer (due to improved thermal properties) and by distributing the reactant uniformly throughout the reactor bed [37].

Methane and ethylene yields increased from 5 to 14 mole % and 23–44 mole %, respectively over the same range of feed concentration. At high concentrations, the reactants would flood the catalyst active sites and affect the gasification to the highest gas products. The carbon balance showed that complete conversion of glycerol to gaseous and liquid products was realised even for the highest feed concentrations tested (30 wt% glycerol) at 550 °C using the reported catalyst. Fig. 11 shows that the liquid product decreases from 44 to 22 wt% when glycerol feed concentrations increases from 2 to 30 wt%, respectively. Conversely, the gas yield increased significantly from 55 to 77 wt% in the same range largely as a result of increased light hydrocarbon and CO yields.

3.3.5. Effect of time online on gas yield

The effect of time online was studied by monitoring the gas product yield for up to 9 h to provide important data about catalyst stability. It can be seen in Fig. 12 that hydrocarbon yields increased with time online; methane and ethylene yield increased slowly from 13 to 16 mole % and 41–52 mole%, respectively. The increase in methane may have resulted from gas–solid reactions that would be occurring (C + $2H_2 \rightarrow CH_4$) due to char formation. On the other hand, CO and H_2 remain stable during the first 3–4 h; they then both decrease thereon from 34 to 28 mole % for H_2, and from 5 to 2 mole % for CO. This could also be due to a decrease of active sites resulting from the deposition of coke on the catalyst particles or thermal transformation of the catalyst as evidenced by deposition of fragments on the catalyst surface (refer to Fig. 3). Carbon monoxide and hydrogen can also produce methane through methanation side reactions: CO + $3H_2 \rightarrow CH_4 + H_2O$ and $CO_2 + 4H_2 \rightarrow CH_4 + 2H_2O$ and may contribute for the low H_2 yield. Both of these reactions are exothermic and are favoured by lower temperature as compared to steam reforming of methane (SRM), which would occur at high temperature (700–800 °C). Evidence of char formation was revealed also by ESEM-EDS analysis of the fresh and used sample after 9 h on-stream, which gave carbon dry catalyst weight percentages of 5.2 and 5.5 wt%, respectively; representing an accumulation of 0.3 wt% of char. However as seen in
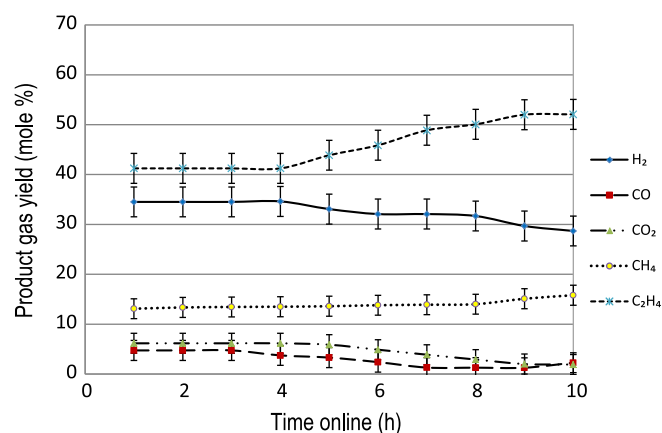

Fig. 12. Effect of time online on gas product yield for 20 wt% glycerol. T = 500 °C, P = 235 barg and WHSV = 125 h^{-1}.

Section 3.3.3, temperature is a salient parameter for char formation, especially over prolonged use.

3.4. Liquid product analysis of CSCWG of glycerol

Liquid product analysis showed that the main liquid products were <11 wt% cumulatively. These were methanol, allyl alcohol, ethanol, formaldehyde, acrolein, acetaldehyde and propionaldehyde. These products were also found in other studies [6,11]. The wide variety of products reflects the complexity of the reaction mechanisms involved in the hydrothermal decomposition of glycerol, which can be summarised in the coexistence of competing ionic and free radical pathways. The liquid products were formed both in the subcritical and supercritical conditions; their composition and yield are discussed in a separate paper.

4. Conclusions

The catalytic gasification of glycerol was studied under sub and supercritical water conditions (170—250 barg and 400—550 °C) using an iron-chromium oxide (91:9 wt%) catalyst. Pure glycerol was converted (up to 98% conversion) at 500 °C into gaseous products largely containing hydrogen, methane and ethylene. In addition, useful condensates, such as allyl alcohol and methanol were also obtained. Complete conversion of glycerol was achieved at 550 °C as indicated by no trace of glycerol in the liquid sample analysis. In comparison to other gasification process, the gaseous product was relatively clean with only five components in the composition (H_2, CO, CO_2, CH_4 and C_2H_4) with low traces of char (<2.7 wt% after 172 h and 0.3 wt% after 9 h) in the overall products. The temperature and glycerol feed concentration largely affected the gaseous product yield. 550 °C is needed to achieve high yields of gaseous products for up to 30% wt pure glycerol concentration. However, pressure was found to have a moderate effect on the gas composition and yield. H_2 and CO_2 yield increased with pressure as a result of promoting the WGS reaction. The hydrogen and syngas yields were as high as 62 and 64 mole % respectively, with a minimum mole ratio H_2:CO of 4:1 largely attributed to high yield of H_2. The highest yields of light hydrocarbons were, methane (22 mole %) and ethylene (69 mole %), which could be used as fuel gas with medium heating value for producing electricity through a turbine or SOFC or reforming to syngas. The iron oxide catalyst exhibited potent stability after 9 h of operation, but was not selective at promoting the production 2:1 ratio of H_2:CO at the reported conditions. 2:1 ratio of H_2:CO is the desired syngas composition for FTS into mixed alcohols.

Acknowledgements

Nomenclature and abbreviations

$C_{g,\ i}$	concentration of the component (i) in the gas sample
C_S	concentration of the external standard
A_i	peak areas of the component (i) in the gas sample
A_S	peak areas of the external standard
$C_{l,\ i'}$	concentration of the component (i′) in the liquid sample
$A_{l,\ i'}$	peak areas of the component (i′) in the liquid sample
$A_{S'}$	peak areas of the internal standard in the liquid sample
y	intercept of the linear calibration equation
P	pressure, barg
T	temperature, °C
F	feed flow rate, ml/min
τ	residence time, s
CSCWG	catalytic supercritical water gasification
SRM	steam reforming of methane
SOFC	solid oxide fuel cell
LHSV	liquid hourly space velocity

References

[1] Wendisch VF, Lindner SN, Meiswinkel TM. Use of glycerol in biotechnological applications; 2011. p. 305—34.
[2] Duane TJ, Katherine AT. Environ Prog 2007;26:338—48.
[3] Yuksel A, Koga H, Sasaki M, Goto M. Hydrothermal electrolysis of glycerol using a continuous flow reactor. Ind Eng Chem Res 2010;49:1520—5.
[4] Montané D, May A, Salvadó J. Catalytic gasification of glycerol in supercritical water for hydrogen production. WHEC 2010;5:16—21.
[5] Van Bennekon JG, Assink D, Heeres HJ. Reforming of methanol and glycerol in supercritical water. J Supercritical Fluids 2011;58:99—113.
[6] May A, Salvedo J, Torras C, Montane D. Catalytic gasification of glycerol in supercritical water. Chem Eng J 2010;160:751—9.
[7] Chakinale AG, Brilman DWF, Van Swaaij WPM, Kerstan SRA. Catalytic and non-catalytic supercritical water gasification of microalgae and glycerol. Ind Eng Chem Res 2010;49:1113—22.
[8] Dileo GJ, Neff ME, Kim S, Savage PE. Supercritical water gasification of phenol and glycine as models for plant and protein biomass. Energy Fuels 2008;22:871—7.
[9] Xiaodong X, Yukihiko M, Jonny S, Michael J. Carbon-catalysed gasification of organic feedstock in supercritical water. Ind Eng Chem Res 1996;35:2522—30.
[10] Iriondo A, Barrio VL, Cambra JF. H_2 production from glycerol over Ni/Al$_2$O$_3$ modified by Mg, Zr, Ce or La. Top Catal 2008;49:46—58.
[11] Buhler W, Dinjus WE, Ederer HJ, Kruse A, Mas C. Ionic reactions and pyrolysis of glycerol as competing reaction pathways in near-and supercritical water. J Supercritical Fluids 2002;22:37—53.
[12] Xu D, Wang S, Hu X, Chen C, Zhang Q. Catalytic gasification of glycerine and glycerol in supercritical water. Int J Hydrogen Energy 2009;34:5357—64.
[13] Voll FAP, Rossi CCRS, Silva C, Guirardello R, Sourza ROMA, Cabrall VF, et al. Thermodynamic analysis of supercritical water gasification of methanol, ethanol, glycerol, glucose and cellulose. Int J Hydrogen Energy 2009.
[14] Valliyappan T, Ferdous D, Bakhshi NN, Dalai AK. Production of hydrogen and syngas via steam gasification of glycerol in a fixed-bed reactor. Top Catal 2008;49:59—67.
[15] Osada M, Sato T, Watanabe M, Adshiri T, Arai K. Energy fuel 2004;18:327—33.
[16] Hao X, Guo L, Zhang X, Guan Y. Proceedings WHEC2010 297. Chem Eng J 2005;110:57—65.
[17] Guo Y, Wang SZ, Xu DH, Gong YM, Ma HH, Tang XY. Review of catalytic supercritical water gasification for hydrogen production from biomass, 14(2010): 334—43.
[18] Douglas CE, Gary GN, Todd RH, Butner S, Alan HZ, Mark H. Chemical processing in high-pressure aqueous environments, process development for catalytic gasification of wet biomass feedstocks. Ind Eng Chem Res 2004;43:1999—2004.
[19] Armbruster U, Martin A, Krepel A. Hydrolysis and oxidative decomposition of ethyl acetate in sub- and super-critical water. Appl Catal B Environ 2001;31:263—73.
[20] J Antal M, Allen S, Lichwa J, Schulman D, Xu X. Hydrogen production from high-moisture content biomass in supercritical water. In: proceedings of the US-DOE hydrogen program review 1999. p. 2—24. NREL/CP-570-26938.
[21] Espinoza RL, Steynberg AP, Jager B, Vosloo AC. Low temperature Fischer—Tropsch synthesis from a Sasol perspective. Appl Catal A Gen 1999;186:13.
[22] Steynberg AP, Espinoza RL, Jager B, Vosloo AC. High temperature Fischer—Tropsch synthesis in commercial practice. Appl Catal A Gen 1999;186:41.
[23] Mozaffarian M, Deurwaarder EP. Syngas production by supercritical water gasification of biomass; 2004. p. 3—71.
[24] Goula MA, Kontou SK, Tsiakaras PE. Hydrogen production by ethanol steam reforming over a commercial Pd/_-Al2O3 catalyst. Appl Catal B Environ 2004;49:135—44.
[25] Haryanto A, Fernando S, Murali N. current status of hydrogen production techniques by steam reforming of ethanol, a review. Energy Fuels 2005;19:2098—106.
[26] San SH, Park D, Duffy GJ, Edwards JH, Roberts DG, Llyushechkin A, et al. Kinetics of high-temperature water-gas shift reaction over two iron-based commercial catalysts using simulated coal-derived syngas. Chem Eng J 2009;146:148—54.
[27] Paul AW, Jefferson WT. Fundamental kinetics of methane oxidation in supercritical water. Energy Fuels 1991;5:411—9.
[28] Antal MJ, Allen SG, Schulman D, Xu XD, Divilio RJ. Biomass gasification in supercritical water. Ind Eng Chem Res 2000;39:4040—53.
[29] Demirbas A. Progress and recent trends in biofuels. Prog Energy Combust Sci 2007;33:1—18.
[30] Richard KH, Jefferson WT. Oxidation kinetics of carbon monoxide in supercritical water. Energy Fuels 1987;1:417—23.

[31] Matsumuraa Y, Minowab T, Biljana P, Kerstenc SRA, Wolter P, Willibrordus PM, et al. Biomass gasification in near- and supercritical water: status and prospects. Biomass and Bioenergy 2005;29:269–92.

[32] Coll R, Salvado J, Farriol X, Montane D. Steam reforming model compounds of biomass gasification tars: conversion at different operating conditions and tendency towards coke formation. Fuel Process Technol 2001;74:19–31.

[33] Buhler W. Modelling of the reaction behaviour of glycerol in sub-and super-critical water, science. Reports of the Research Center Karlsruhe FZKA 6553. Research-Local info Karlsruhe; 2000.

[34] Savage PE. Organic chemical reactions in supercritical water. Chem Rev 1999;99:603–21.

[35] Adam JB, Pant KK, Ram BG. Hydrogen production from glycerol by reforming in supercritical water over Ru/Al$_2$O$_3$ catalyst. Fuel 2008;87: 2956–60.

[36] Xue E, O'Keeffe M, Ross JRH. Water–Gas shift conversion using a feed with a low steam to carbon monoxide ratio and containing sulfur. Catal Today 1996;30:107–18.

[37] Hirai T, Ikenaga NO, Miyake T, Suzuki T. Production of hydrogen by steam reforming of glycerin on ruthenium catalyst. Energy Fuels 2005;19: 1761–2.

[38] Chun-Jiang J, Ling-Dong S, Feng L. Large-scale synthesis of single-crystalline iron oxide magnetic nanorings. J Am Chem Soc 2008;130(50):16968–77.